https://doi.org/10.1093/plphys/kiac051 PLANT PHYSIOLOGY 2022: 189: 84–98

Plant Physiology®

Research Article

Two major metabolic factors for an efficient NADP-malic enzyme type C_4 photosynthesis

Honglong Zhao,[1] Yu Wang ,[2] Ming-Ju Amy Lyu [1] and Xin-Guang Zhu [1,*,†]

1 Center of Excellence for Molecular Plant Sciences, Chinese Academy of Sciences, Shanghai 200032, China
2 The Carl R. Woese Institute for Genomic Biology, University of Illinois Urbana-Champaign, Champaign, Illinois 61801, USA

*Author for correspondence: zhuxg@cemps.ac.cn
†Senior author

H.L.Z., and X.G.Z. designed this project. H.L.Z. and Y.W. conducted the simulations. H.L.Z., M.J.L., and X.G.Z. performed the analyses. H.L.Z. and X.G.Z. wrote the paper. All the authors edited the manuscript.
The author responsible for distribution of materials integral to the findings presented in this article in accordance with the policy described in the Instructions for Authors (https://academic.oup.com/plphys/pages/general-instructions) is Xin-Guang Zhu (zhuxg@cemps.ac.cn).

Abstract

Compared to the large number of studies focused on the factors controlling C_3 photosynthesis efficiency, there are relatively fewer studies of the factors controlling photosynthetic efficiency in C_4 leaves. Here, we used a dynamic systems model of C_4 photosynthesis based on maize (*Zea mays*) to identify features associated with high photosynthetic efficiency in NADP-malic enzyme (NADP-ME) type C_4 photosynthesis. We found that two additional factors related to coordination between C_4 shuttle metabolism and C_3 metabolism are required for efficient C_4 photosynthesis: (1) accumulating a high concentration of phospho*enol*pyruvate through maintaining a large PGA concentration in the mesophyll cell chloroplast and (2) maintaining a suitable oxidized status in bundle sheath cell chloroplasts. These identified mechanisms are in line with the current cellular location of enzymes/proteins involved in the starch synthesis, the Calvin–Benson cycle and photosystem II of NADP-ME type C_4 photosynthesis. These findings suggested potential strategies for improving C_4 photosynthesis and engineering C_4 rice.

Introduction

With the global population growth, improved economic status, and changing climate, securing food supply is still a major issue facing our society. Increasing productivity of both C_3 and C_4 crops is needed to realize the desired food security (Ray et al., 2013; Hunter et al., 2017). Much effort has been made to improve photosynthetic efficiency of C_3 plants (Long et al., 2015; Shen et al., 2019; South et al., 2019; López-Calcagno et al., 2020). Comparatively, the efforts to improve photosynthetic efficiency in C_4 plants are lacking.

To increase photosynthesis in C_4 plants, some individual enzymes limiting C_4 photosynthesis have been identified by calculating the control coefficient of each enzymatic step. For example, carbonic anhydrase (CA; von Caemmerer et al., 2004; Studer et al., 2014), phosphoenolpyruvate carboxylase (PEPC; Boyd et al., 2015), and pyruvate orthophosphate dikinase (PPDK; Wang et al., 2008) may have relatively large control coefficients on the C_4 photosynthetic CO_2 fixation rate (A; von Caemmerer and Furbank, 2016). Additionally, Rubisco is identified as a key limiting factor for C_4 photosynthesis (von Caemmerer et al., 1997; Wang et al., 2014a, 2014b). Salesse-Smith and collaborators increased Rubisco activity in maize (*Zea mays*) by the overexpression of Rubisco subunits together with the assembling chaperone RUBISCO ASSEMBLY FACTOR 1, which results in increased photosynthesis and biomass in transgenic maize compared with those in the wild-type (WT) (Salesse-Smith et al., 2018). All these studies show that there is room to further enhance

Received July 29, 2021. Accepted January 15, 2022. Advance access publication February 15, 2022

the photosynthetic CO_2 uptake rate in C_4 plants (Matsuoka et al., 2001; von Caemmerer and Furbank, 2016).

Besides improving the photosynthetic efficiency of C_4 plants, great efforts have been invested into engineering C_3 plants to perform C_4 photosynthesis. The C_4 plants usually have higher photosynthetic energy conversion efficiency compared to C_3 plants, as a result of having a CO_2 concentration mechanism (CCM; Zhu et al., 2008), which functions as a CO_2 "pump," that is, concentrating CO_2 around Rubisco in the bundle sheath cells (BSCs) and inhibiting photorespiration (Sage, 2004). Introducing the CCM of C_4 photosynthesis into C_3 crops through genetic engineering can potentially enhance yield of C_3 crops by 50% (Matsuoka et al., 2001; Hibberd et al., 2008; Covshoff and Hibberd, 2012; Furbank et al., 2015). Historically, hybridization between C_3 and C_4 plants has been used as a strategy to realize this goal, as summarized by Brown and Bouton (1993). Unfortunately, this effort did not succeed largely due to the difficulty of obtaining stable genetically inheritable germplasm after hybridization. Later, single enzymes of C_4 photosynthesis and multigene combinations for the NADP-malic enzyme (NADP-ME) type C_4 CCM were introduced into rice (*Oryza sativa* ; Fukayama et al., 2001, 2003, 2006; Tsuchida et al., 2001; Taniguchi et al., 2008), which culminated in the incorporation of a single-cell C_4 photosynthetic pathway (Miyao et al., 2011) or the two-cell NADP-ME type C_4 photosynthetic pathway into rice (Ermakova et al., 2020). Unfortunately, so far, in transgenic plants with enhanced expression of CCM-related enzymes, photosynthesis did not increase (Ku et al., 2001; Miyao et al., 2011; Ermakova et al., 2020). Two recent reports showed that a partial NADP-ME type C_4 photosynthetic biochemical pathway has been successfully constructed in rice (Lin et al., 2020; Ermakova et al., 2021). The enzymes simultaneously overexpressed in the rice plants include PEPC, PPDK, NADP-ME, and malate dehydrogenase (Lin et al., 2020). Additionally, a two-cell prototype by overexpressing the four C_4 cycle enzymes above and CA in rice with the specific cellular compartmentations has also been developed (Ermakova et al., 2021). In both studies, a partial C_4 biochemical pathway has been successfully installed (Lin et al., 2020; Ermakova et al., 2021). Since there are no remarkable malate decarboxylation fluxes detected in their work, the whole cycle of C_4 CCM in transgenic rice seems unfunctional.

The lack of detectable C_4 fluxes implies that there might be other major features that are missed in the current C_4 engineering effort. The lack of a complete C_4 cycle in the engineered plants might be due to a lack of the sufficient metabolite transporter activities, existence of barriers preventing CO_2 leakage from BSCs to mesophyll cells (MCs), and a lack of a sufficient number of chloroplasts in BSC (Bchl; Lin et al., 2020). A number of recent studies suggest some metabolic features which may be equally important for the operation of a complex metabolic pathway. For example, maintaining sufficiently high concentrations of the intermediates is a major factor to ensure a sufficiently high metabolite flux through a system (Antonovsky et al., 2016; Barenholz et al., 2017). Furthermore, to ensure a highly efficient system, simple over-expression of enzymes in the metabolic pathway is not sufficient. For example, overexpressing transketolase in the Calvin–Benson cycle (CBC) leads to the disruption of the metabolic coordination for triose phosphate (T3P) available for different metabolism pathways, ultimately inhibiting plant growth (Khozaei et al., 2015). Our recent theoretical analysis shows that the excess enzymatic capacity of some steps in the CBC can reduce metabolic network efficiency as a result of an imbalanced distribution of shared metabolites among different sub-cycles (Zhao et al., 2020). Considering that C_4 photosynthesis requires highly efficient coordination between BSC and MC (Stitt and Zhu, 2014), the question arising here is: are there metabolic features that are required for C_4 photosynthesis that have been missed in all current C_4 engineering efforts?

This study aims to identify the metabolic features required to gain an efficient C_4 photosynthesis, which will not only be crucial for the current efforts of improving photosynthetic efficiency of contemporary C_4 plants, but also provide important targets for consideration in the current efforts of engineering C_3 plants to perform C_4 photosynthesis.

Results

Model analysis

Although CO_2 is initially fixed by PEPC in C_4 photosynthesis, it is ultimately fixed by Rubisco. In other words, the C_4 photosynthetic rate can be calculated based on the reaction catalyzed by Rubisco. Net photosynthetic CO_2 fixation rate (A) is calculated by the following formula (Farquhar et al., 1980):

$$A = v_c - 0.5 * v_o - Rd \quad \ldots (1)$$

where v_c and v_o represent the rates of RuBP (ribulose -1,5-bisphosphate) carboxylation and oxygenation catalyzed by Rubisco, respectively. *Rd* represents the CO_2 release rate from day respiration. Its value is assumed to be 1 μmol m^{-2} s^{-1} as in the previous model (Wang et al., 2014a, 2014b). According to the Michaelis–Menten kinetics, the v_c and v_o are described as (Wang et al., 2014a, 2014b):

$$v_c = V_{cmax} * \frac{[RuBP]_{Bchl}}{[RuBP]_{Bchl} + KM_{RuBP}} * \frac{[CO_2]_{Bchl}}{[CO_2]_{Bchl} + KM_{CO_2} * \left(1 + \frac{[O_2]_{Bchl}}{Ki_{O_2}}\right)} \quad \ldots (2)$$

$$v_o = V_{omax} * \frac{[RuBP]_{Bchl}}{[RuBP]_{Bchl} + KM_{RuBP}} * \frac{[O_2]_{Bchl}}{[O_2]_{Bchl} + KM_{O_2} * \left(1 + \frac{[CO_2]_{Bchl}}{Ki_{CO_2}}\right)} \quad \ldots (3)$$

$$V_{omax} = 0.11 * V_{cmax} \quad \ldots (4)$$

where V_{max} is the maximal velocity of Rubisco, KM_{RuBP} is the apparent Michaelis–Menten constant of Rubisco for RuBP; KM_{CO2} and KM_{O2} are the Michaelis–Menten

constants of Rubisco for CO_2 and O_2, respectively; Ki_{CO2} and Ki_{O2} are the inhibition constants of CO_2 and O_2, respectively; the subscript "Bchl" means chloroplast in the BSC.

According to Equations (1–4),

$$A = V_{cmax} * \frac{[RuBP]_{Bchl}}{[RuBP]_{Bchl} + KM_{RuBP}} * \left(\frac{[CO_2]_{Bchl}}{[CO_2]_{Bchl} + KM_{CO_2} * \left(1 + \frac{[O_2]_{Bchl}}{Ki_{O_2}}\right)} - \frac{0.11 * [O_2]_{Bchl}}{[O_2]_{Bchl} + KM_{O_2} * \left(1 + \frac{[CO_2]_{Bchl}}{Ki_{CO_2}}\right)} \right) - Rd \quad \ldots (5)$$

We define that:

$$f([RuBP]) = \frac{[RuBP]_{Bchl}}{[RuBP]_{Bchl} + KM_{RuBP}} \quad \ldots (6)$$

$$f([CO_2]) = \frac{[CO_2]_{Bchl}}{[CO_2]_{Bchl} + KM_{CO_2} * \left(1 + \frac{[O_2]_{Bchl}}{Ki_{O_2}}\right)} - \frac{0.11 * [O_2]_{Bchl}}{[O_2]_{Bchl} + KM_{O_2} * \left(1 + \frac{[CO_2]_{Bchl}}{Ki_{CO_2}}\right)} \quad \ldots (7)$$

Such that A is calculated as (Figure 1):

$$A = V_{cmax} * f([RuBP]) * f([CO_2]) - Rd \quad \ldots (8)$$

In this study, we aimed to study the inherent biochemical requirements to gain an efficient NADP-ME type C_4 photosynthesis. So we conducted the simulations under both high-light and high-CO_2 level where there is no limitation of either light or CO_2. Specifically, we assume an irradiance of 1500μmol m^{-2} s^{-1}, an O_2 levels of 21% and a $[CO_2]$ of 800 ppm. The rate of the Rubisco catalyzed reaction is determined by maximal Rubisco carboxylation capacity, the concentrations of RuBP, CO_2, and O_2 concentrations around Rubisco (Equation (8)). Based on the transformed Michaelis–Menten equation ($\frac{v}{Vmax} = \frac{\frac{[S]}{Km}}{\frac{[S]}{Km}+1}$), the relationship between enzyme and its substrates ($\frac{v}{Vmax}$ versus $\frac{[S]}{Km}$) is proposed as a measure of the limiting status for an enzymatic reaction (Fendt et al., 2010; Zhao et al., 2020). We used the same method as in Zhao et al. (2020) to identify enzymes which show biphasic responses to changing enzyme activities and study the underlying metabolic basis of the biphasic responses.

Increasing the enzymatic capacity related to C_3 metabolism may inhibit NADP-ME type C_4 photosynthesis

We used a dynamic systems model for the NADP-ME type C_4 photosynthesis for the analysis (Wang et al., 2014a, 2014b). We first simulated the effects of increasing values of individual parameters on photosynthetic rates (A). Altogether 38 parameters in this model (36 V_{max} of enzymatic reactions and 2 parameters associated with plasmodesmata) were perturbed (Figure 2; Supplemental Figure S1). Our results show that 6 out of 38 parameters have biphasic effects on the photosynthetic rates (Figure 2). These parameters include the maximal velocities of four enzymatic reactions and two parameters related to plasmodesmata. Following Zhao et al. (2020), we named enzymes producing biphasic responses as elements producing biphasic response (EPBR). The EPBR enzymes identified are PGAK-GAPDH in either chloroplast in MC (Mchl) or the Bchl, FBP aldolase, and FBPase in Bchl (Figure 2, A and B). The other 32 parameters produce nonbiphasic responses (Supplemental Figure S1). There are three types of nonbiphasic responses with the increase in enzyme activities: (1) first increase then a plateau; (2) first decrease and then a plateau; and (3) nonresponsive (Supplemental Figure S1).

The efficiency of C_4 photosynthesis is determined by both the CBC for RuBP regeneration and C_4 cycle for CO_2 pumping (Figure 1). Rubisco catalytic capacity is maintained at its default value in our univariable analysis for EPBRs, so the changes of chloroplastic [RuBP] and $[CO_2]$ in BSC are two factors contributing to the changes in photosynthetic rates in our perturbation experiments (Figure 1; Equation 8). Next, we analyzed the impacts of EPBRs' activities on the limitations of chloroplastic [RuBP] and $[CO_2]$ in BSC to photosynthesis. Thereafter, we analyzed the biochemical mechanisms underlying the influence of EPBRs on the operations of the CBC and C_4 cycle.

Excess capacity of EPBR limits the efficiency of the RuBP regeneration cycle or the C_4 cycle

To elucidate the mechanistic basis of biphasic responses of NADP-ME type C_4 photosynthesis to the increase in each EPBR capacity (Figure 2), we first determined the limiting factor for photosynthetic CO_2 uptake rate, that is, whether it is [RuBP] or $[CO_2]$ or Rubisco activity that limits A under a particular perturbation. We plotted the enzyme–substrate relationship ([S]/KM versus v/V_{max}) of Rubisco under a wide range of activities of each EPBR (Figure 3). Each subgraph is separated into three regions by two vertical dashed lines (Figure 3). For the left and right dashed lines, [S]/KM are 0.04 and 40 (Figure 3), respectively. These two values are based on previous studies (Fendt et al., 2010; Zhao et al., 2020). Three regions from left to right represent three limiting stages of Rubisco carboxylation (Figure 3), including the substrate limiting stage (the ratio of [S]/KM is <1 in the left region), enzymatic capacity limiting stage (the ratio of [S]/KM is >1 in the right region), and substrate and enzymatic capacity co-limiting stage (the ratio of [S]/KM is comparable to 1 in the middle region) (Figure 3; Fendt et al., 2010). The influence of perturbing activities of EPBRs on [RuBP], $[CO_2]$, and A (Figure 3, B, D, F, H, J, and L) are shown in Figure 3. During the perturbations, the default activity of each individual EPBR was changed from the range of 0.01- to 1,000-fold (the color bar in Figure 3). With the increase in activity of PGAK-$GAPDH_{Bchl}$, the ratio of [RuBP]/$KmRuBP_{app}$ increased first and then decreased (Figure 3A),

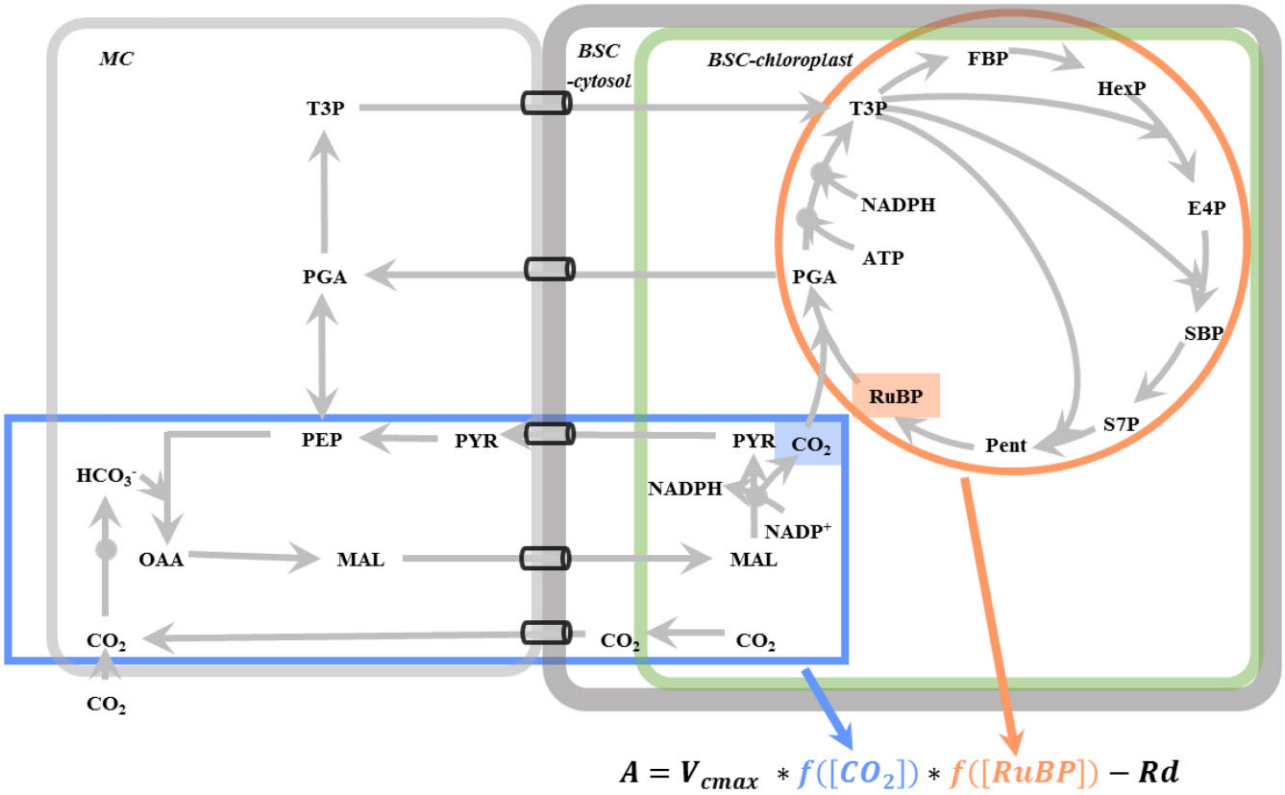

Figure 1 A simplified metabolic diagram of NADP-ME type C_4 photosynthesis. CO_2 is ultimately fixed by Rubisco carboxylation. Under a photosynthetic photon flux density of 1,500 μmol m^{-2} s^{-1}, a CO_2 concentration of 800 ppm and an O_2 level of 21%, the net photosynthetic CO_2 fixation rate (*A*) is determined by the concentrations of CO_2 (blue square) and RuBP (orange square) around Rubisco in the Bchl. The operation efficiencies of C_4 cycle (metabolic module in the blue box) and CBC (metabolic module in the orange circle) determine the efficiencies of CO_2 concentrating and RuBP generation, respectively. V_{max} is the maximal velocity of Rubisco. *f([RuBP])* and *f([CO_2])* are the functions shown in Equations (6) and (7), respectively. *Rd* means the dark respiration rate.

meanwhile $[CO_2]/KmCO_{2app}$ kept rising (Figure 3B). With the increase in activity of $FBPA_{Bchl}$ or $FBPase_{Bchl}$, ratios of both $[RuBP]/KmRuBP_{app}$ (Figure 3, C and E) and $[CO_2]/KmCO_{2app}$ (Figure 3, D and F) increased first and then decreased. With the increase in activity of PGAK-$GAPDH_{Mchl}$, the ratio of $[RuBP]/KmRuBP_{app}$ kept increasing (Figure 3G), meanwhile $[CO_2]/KmCO_{2app}$ kept decreasing (Figure 3H).

Plasmodesmata area proportion and plasmodesmata length are two factors determining the diffusion capacity of plasmodesmata between MC and BSC (Wang et al., 2014a, 2014b). According to the diffusion equation as in (Wang et al., 2014a, 2014b), the metabolites diffusion capacity between BSC and MC through plasmodesmata is positively associated with the proportion of plasmodesmata in the BSC–MC interface and is negatively associated with plasmodesmata length. In our in silico perturbation experiments, we increased the diffusion capacity of plasmodesmata, either by increasing plasmodesmata area proportion (as shown by the gradual change of color in Figure 3, I and J from blue to yellow) or by decreasing plasmodesmata length (as shown by the gradual change in color in Figure 3, K and L from yellow to blue). Results show that, with the increase in plasmodesmata diffusion capacity, the ratio of $[RuBP]/Km_{RuBPapp}$ keeps increasing (Figure 3, I and K) and $[CO_2]/KmCO_{2app}$ decreases (Figure 3, J and L) in general.

Figure 3 shows that, excess activity of PGAK-$GAPDH_{Bchl}$ inhibited the RuBP regeneration (Figure 3A); excess activity of $FBPA_{Bchl}$ or $FBPase_{Bchl}$ decreased the RuBP regeneration (Figure 3, C and E) and CO_2 concentration (Figure 3, D and F); and excess capacity of PGAK-$GAPDH_{Mchl}$ decreased the CO_2 concentration (Figure 3H). Our earlier study showed that the high diffusion ability of plasmodesmata increases the leakage of CO_2 from BSC to the MC and hence prevents the increase of CO_2 concentration in the BSC (Wang et al., 2014a, 2014b). Consistent with previous results, increasing diffusion capacity of plasmodesmata, either through increasing plasmodesmata area proportion (yellow dots in Figure 3I) or decreasing plasmodesmata length (dark blue dots in Figure 3L), resulted in a lower $[CO_2]$ and decreased photosynthetic CO_2 uptake rate (Figure 3, I and L).

In this study, when we conducted the perturbation analysis, we changed activities for enzymes individually, that is, the values of other parameters were not altered except the perturbed parameter. Therefore, the influences on metabolic fluxes should only be due to the changes in metabolite levels.

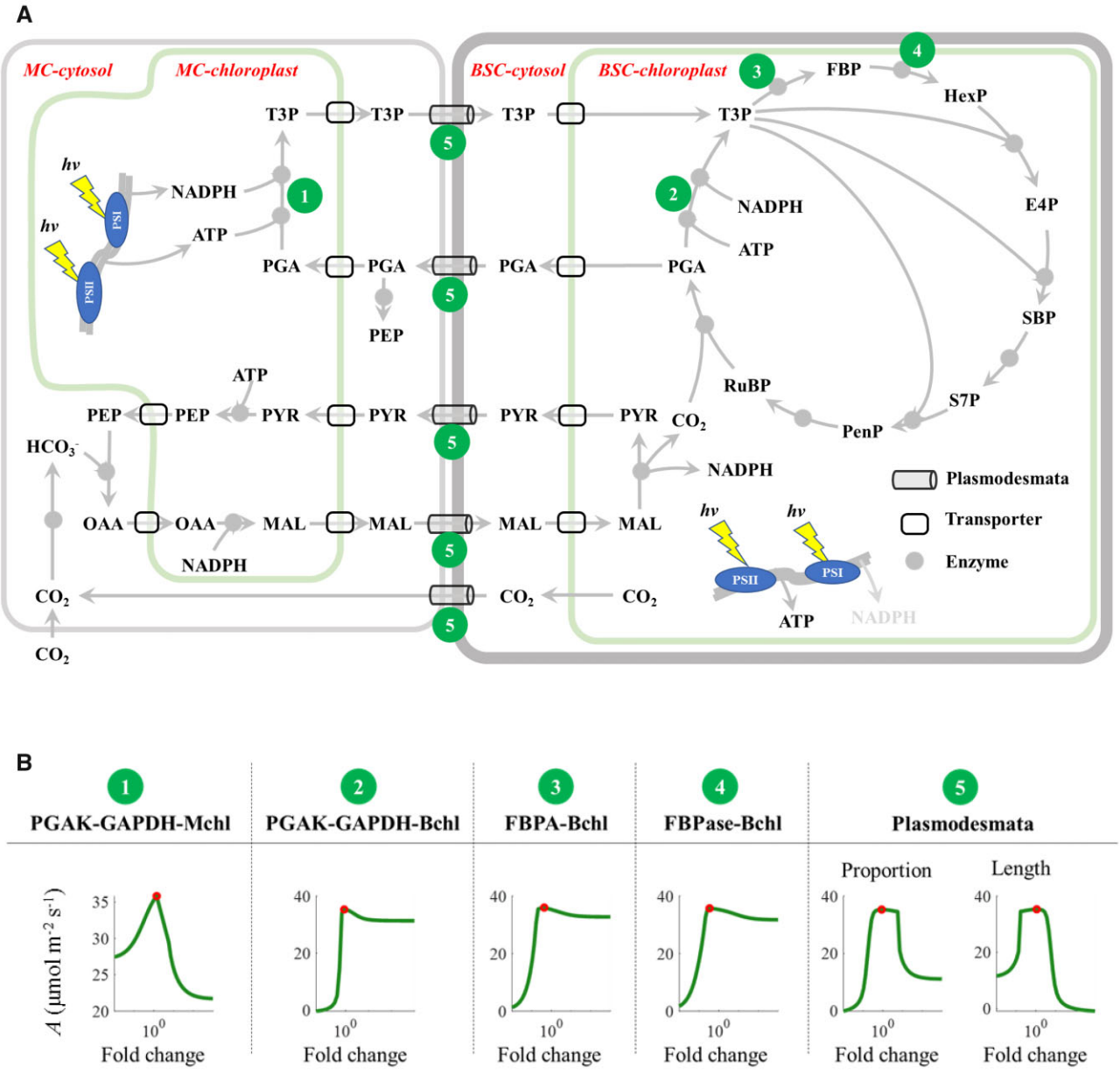

Figure 2 The metabolic processes and their corresponding parameters generating biphasic responses of photosynthetic rates to changes in their value in the NADP-ME type C_4 photosynthesis. In (A), MC represents mesophyll cell, and BSC means bundle sheath cell. In (B) only steps whose V_{max} or feature parameters with biphasic impacts on photosynthetic rates are listed. Mchl indicates that the metabolic process occurs in the chloroplast or membrane of the MCs; Bchl indicates that the process occurs in the chloroplast or membrane of the BSCs; the plasmodesmata proportion represents the ratio of the plasmodesmata to the area of the BSC–MC interface, and its length represents the total cell wall thickness of both MC and BSC cell wall. The *x* axis represents the fold change of a parameter normalized against the parameter value resulting in the maximum net photosynthetic rate.

A suitable PGAK-GAPDH activity in MCs is required for efficient NADP-ME C_4 photosynthesis

To explore why a suitable PGAK-GAPDH activity in Mchl is needed for an efficient NADP-ME type C_4 metabolism, the steady-state concentrations of individual metabolites in the CBC and CCM are plotted against the V_{max} of Mchl PGAK-GAPDH (Figure 4). We first considered the concentrations of RuBP and CO_2 in Bchl. Before the maximal photosynthetic CO_2 uptake rate (Figures 2, B and 4) is reached, increasing Mchl PGAK-GAPDH increased the RuBP concentration, while it decreased the CO_2 concentration in the Bchl (Figure 4). This indicates that the rising phase of photosynthesis (Figure 2B) is caused by the increased RuBP concentration (Figure 3, G and H). As MC PGAK-GAPDH can translocate ATP and NADPH from MC to BSC for CO_2 assimilation (Hatch and Kagawa, 1976), increasing its activity released the accumulation of PGA in both cell types and increased the pool size of the CBC intermediates in the BSC and consequently increased the RuBP accumulation (Figure 4). After *A* reached its maximal rate, further increase

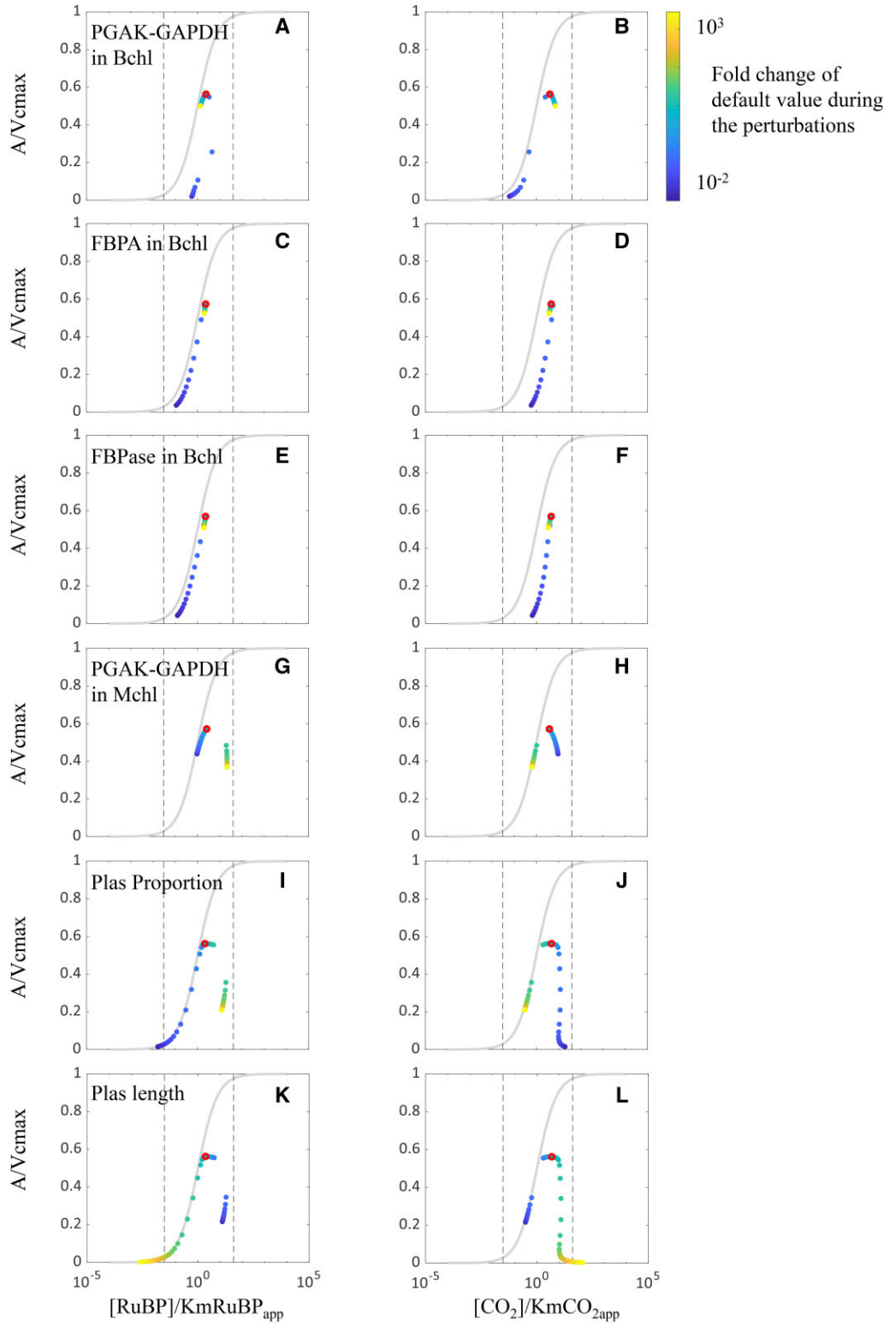

Figure 3 The influence of manipulating enzymes which have a biphasic impact on photosynthetic rates on [RuBP] and [CO_2] and photosynthetic rates. The *y*-axis (A/V_{cmax}) is the ratio of net photosynthesis to the Rubisco carboxylation capacity. The *x*-axis is the ratio of RuBP concentration around Rubisco to the apparent Michaelis–Menten constant of Rubisco for RuBP (subgraphs of A, C, E, G, I, and K in the left column), and the ratio of CO_2 concentration around Rubisco to the Michaelis–Menten constant of Rubisco for CO_2 (subgraphs of B, D, F, H, J, and L in the right column). The color of dots corresponds to fold change of the default value in a C_4 photosynthesis model (Wang et al., 2014a, 2014b). The color from dark blue to yellow represents the fold change range from 0.01 to 1,000. The red dot marks a state which corresponds to the maximal photosynthesis. The perturbated parameters are the enzymatic capacities of the PGAK-GAPDH in the Mchl (A and B), of FBPA in the Bchl (C and D), of FBPase in the Bchl (E and F), of PGAK-GAPDH in the Bchl (G and H), for plasmodesmata proportion (I and J), and plasmodesmata length (K and L).

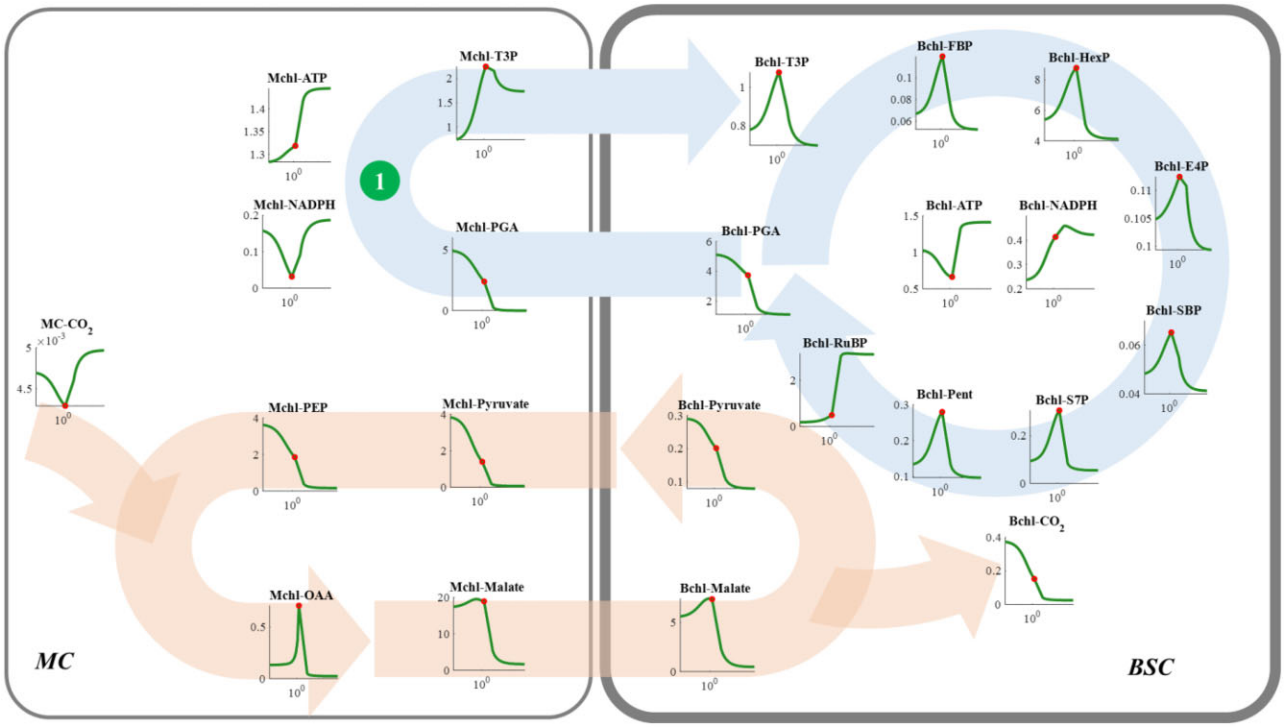

Figure 4 Response curve of metabolite levels in NADP-ME type C_4 photosynthesis to changes in the V_{max} of PGAK-GAPDH in the MCs. The dark green circle numbered ① indicates the location of the PGAK-GAPDH catalyzed reaction in the MC; the circle with light blue curve arrow indicates the CBC; the circle with orange curved arrow indicates the CO_2 concentrating mechanism. The *x*-axis represents the normalized fold changes of the parameter with the 1 representing the parameter resulting in the maximal photosynthetic rate. The *y*-axis represents the metabolite concentration in millimolar. The red dot marks a state which corresponds to the maximal photosynthesis.

in MC PGAK-GAPDH activity decreased the CBC metabolite concentrations except RuBP, and decreased the CO_2 level in the BSC (Figure 4). These simulations suggested the decreased photosynthesis (Figure 2B) was due to the decreased CO_2 level (Figures 3, G and H and 4). In the decreasing phase, concentrations of all metabolites related to CCM were reduced. These perturbations for MC PGAK-GAPDH capacity suggested that the NADP-ME type C_4 photosynthesis switched from RuBP regeneration limitation to CO_2 concentration limitation with increase in the MC PGAK-GAPDH capacity.

Suitable PGAK-GAPDH activity in BSCs is required for efficient NADP-ME C_4 photosynthesis

PGAK can coordinate the ATP consumptions in the CBC (Zhao et al., 2020). Consistent with this role in C_3 photosynthesis, simulations with the dynamic model of NADP-ME type C_4 photosynthesis shows a similar response of the CBC to the increased PGAK-GAPDH in the Bchl (Figure 5; Zhao et al., 2020). When the Bchl PGAK-GAPDH was lower than the optimum, with a decrease in its activity, the CBC efficiency gradually decreased and concentrations of all metabolites in the CBC were decreased. On the contrary, the concentrations of ATP and NADPH in both BSC and MC were increased (Figures 2, B and 5). However, when PGAK-GAPDH activity was higher than the optimum, ATP and NADPH contents in Bchl rapidly decreased and metabolites between PGAK-GAPDH and PRK catalyzed reactions (such as T3P, FBP, HexP, S7P, and Pent) accumulated (Figure 5). Both inadequate and excessive capacities of Bchl PGAK-GAPDH can decrease the RuBP concentration (Figure 5), resulting in a RuBP limitation for Rubisco carboxylation (Figure 3A) and consequently decreased *A* (Figure 2B;Zhao et al., 2020). Additionally, when the Bchl PGAK-GAPDH enzymatic capacity was insufficient, malate level increased (Figure 5), however, the concentrations of metabolites involved in the CCM, that is, pyruvate, phosphoenol pyruvate (PEP), and oxaloacetate (OAA), and also the Bchl CO_2 concentration decreased. These results suggest that inadequate PGAK-GAPDH catalytic capacity decreased RuBP regeneration, repressed malate decarboxylation catalyzed by Bchl NADP-ME, and decreased the donor concentration for CO_2 fixation by PEPC in MC (Figure 5). Although a Bchl PGAK-GAPDH catalytic capacity higher than the optimum reduced the contents of pyruvate (only in MC), PEP, OAA, and malate (in both cell types), the CO_2 concentration in Bchl was maintained at about twice the level of that for the maximal photosynthetic CO_2 uptake rate (red dot in Figure 5). Therefore, these perturbations for Bchl PGAK-GAPDH indicate the decrease of photosynthesis after the maximum

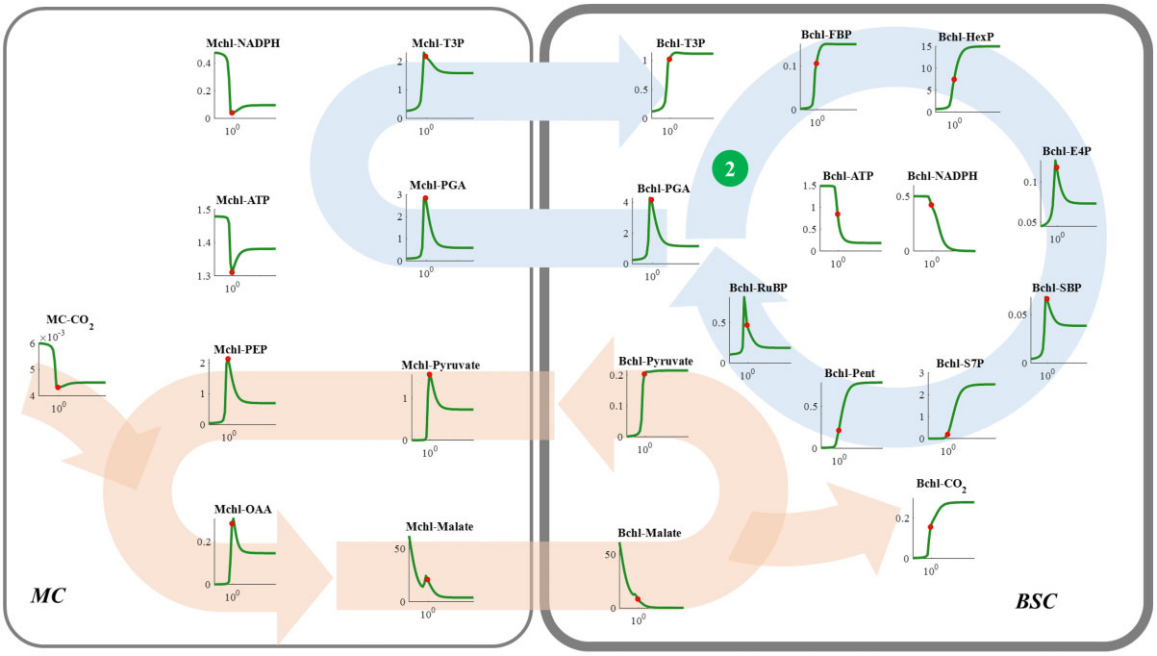

Figure 5 Response curve of metabolite levels in NADP-ME type C_4 photosynthesis to the V_{max} of PGAK-GAPDH (The dark green circle numbered ②) in the BSC. See figure legend for Figure 4 for more details.

PGAK-GAPDH (Figure 2B) can be attributed to the decreased RuBP concentration (Figure 5).

Suitable FBPA and FBPase activities in the Bchl are required for efficient NADP-ME C_4 photosynthesis

Similar to the function of FBPA and FBPase in C_3 photosynthesis, increasing Bchl FBPA or FBPase activity increased the concentrations of the intermediates of the CBC (Figures 6 and 7; Zhao et al., 2020). However, further increase of their activities after the maximal photosynthesis led to a gradual decrease of photosynthesis, since increasing the conversion of T3P to produce FBP and HexP resulted in a shortage of T3P for other reactions in the CBC, ultimately leading to a decrease in the concentrations of other CBC intermediates, including SBP, S7P, Pent, RuBP, PGA, and T3P (Figures 6 and 7; Zhao et al., 2020).

Concentrations of all CCM metabolites decreased when the enzymatic capacity of Bchl FBPA or FBPase was higher than the level required for the maximal photosynthesis (Figures 6 and 7). Although the CO_2 consumption rate declined after the maximal photosynthetic CO_2 uptake rate, the CO_2 concentration in the Bchl dropped (Figures 6 and 7). Therefore, the decrease of photosynthesis after the optimal FBPA and FBPase (Figure 2B) can be attributed to the combined effects of decreased RuBP concentration and the reduced CO_2 concentration (Figures 6 and 7). It indicates that not only the efficiency of CBC, but also that of CCM can be inhibited by an excessive catalytic capacity of Bchl FBPA or FBPase.

Suitable diffusion capacity of plasmodesmata between BSCs and MCs is required for efficient NADP-ME C_4 photosynthesis

The plasmodesmata diffusion capacity is critical for intermediates translocation between BSC and MC, and hence affects the efficiency of C_4 photosynthesis. Increasing the diffusion capacity generates a biphasic photosynthesis response curve of A (Figure 2B;Wang et al., 2014a, 2014b). Since increasing the plasmodesmata area proportion has the same effect on the plasmodesmata diffusion property as decreasing plasmodesmata length, we only analyzed the metabolic mechanisms of increasing plasmodesmata area proportion on C_4 photosynthesis in this sub-session.

With an increase in plasmodesmata area proportion, the RuBP concentration increased (Figure 8), and the BSC CO_2 concentration decreased (Figure 8). This indicates that, before the plasmodesmata area proportion reached an optimum, an increase in photosynthesis with greater plasmodesmata area proportion resulted from an increased RuBP concentration (Figures 3, I and 8). Under these conditions, the limited plasmodesmata diffusion capacity constrained the translocation of intermediates, for example, the movements of PGA and pyruvate from BSC to MC, and the movements of T3P and MAL from MC to BSC. This led to the inhibited capacity of C_3 and C_4 shuttles between MC and MSC (Figure 8), and ultimately decreased NADPH provision for driving the RuBP regeneration in BSC. Although levels of CO_2 and ATP were high in Bchl under these conditions, the intermediate levels in the downstream of

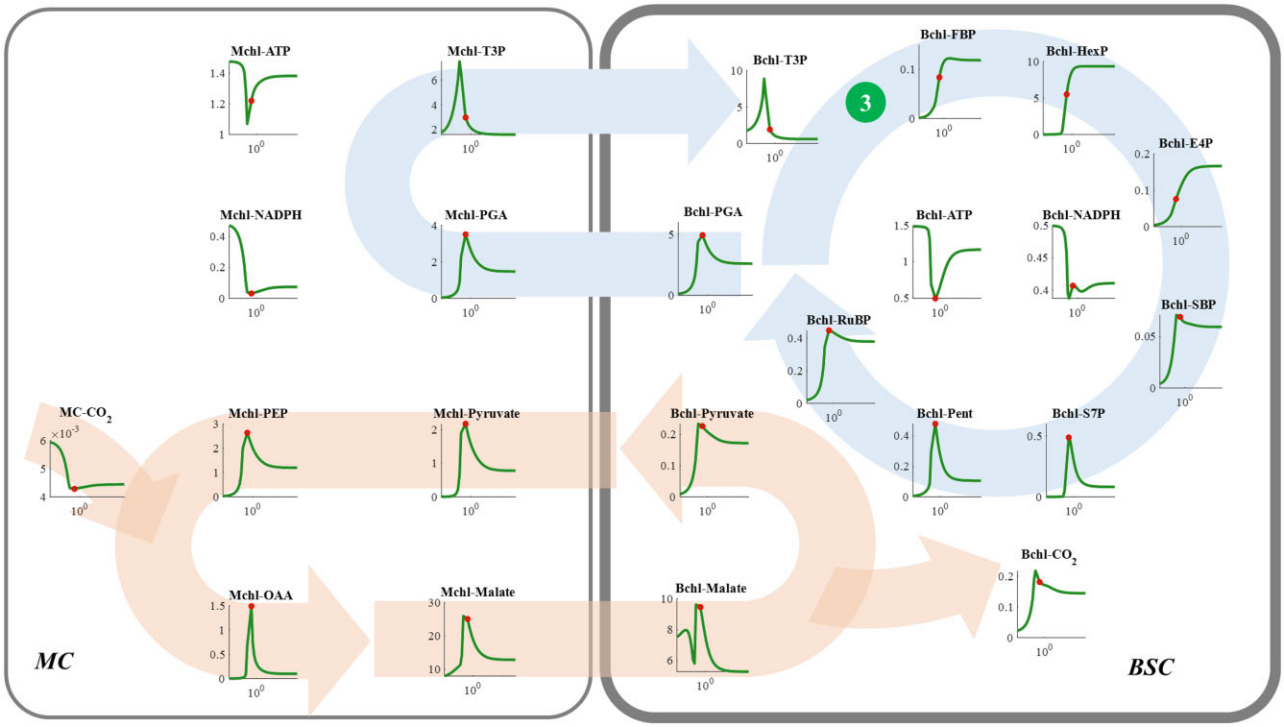

Figure 6 Responses of metabolite levels in NADP-ME type C_4 photosynthetic metabolism to increase of the V_{max} of FBPA (The dark green circle numbered ③) in the BSC. See figure legend for Figure 4 for more details.

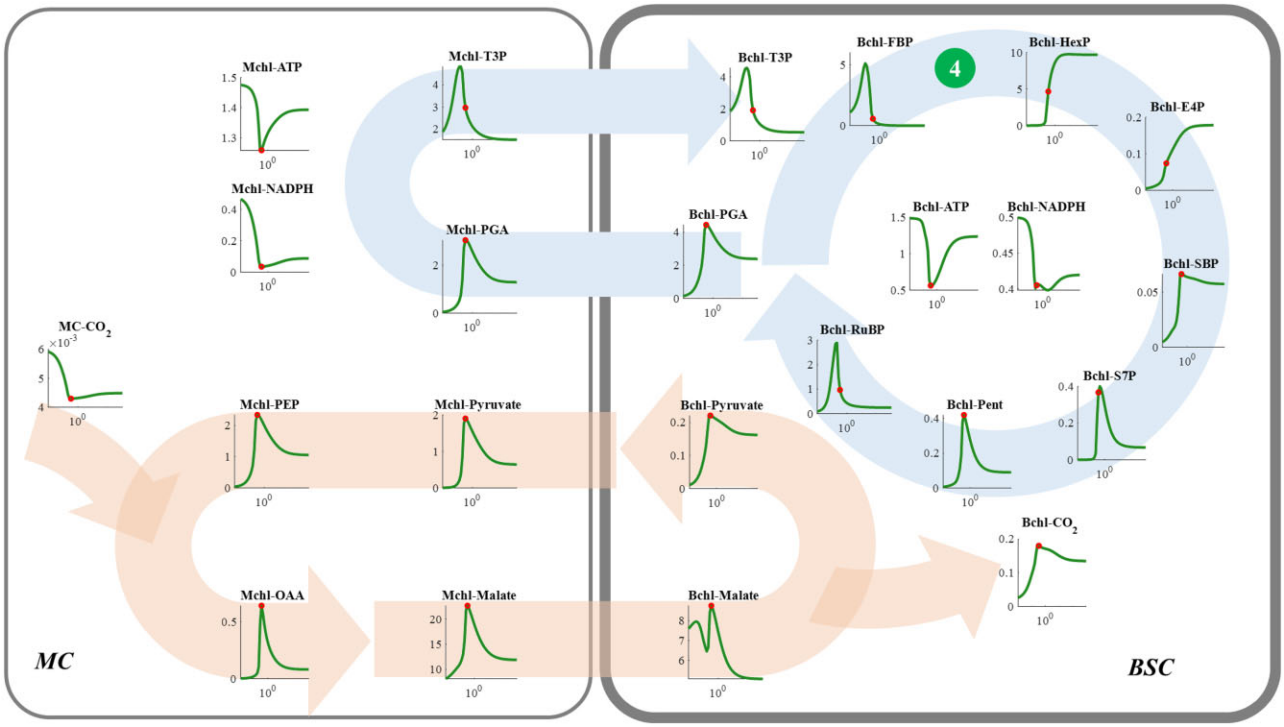

Figure 7 Responses of metabolite levels in NADP-ME type C_4 photosynthetic metabolism to the changes in the V_{max} of FBPase in the BSC (the dark green circle numbered ④). See figure legend for Figure 4 for more details.

PGA reduction and RuBP regeneration in the CBC were low (Figure 8), which ultimately limited NADP-ME type C_4 photosynthetic efficiency (Figure 2).

However, a further increase in the plasmodesmata area proportion after the optimum led to decreased photosynthesis (Figure 2). Different from the reasons above, the

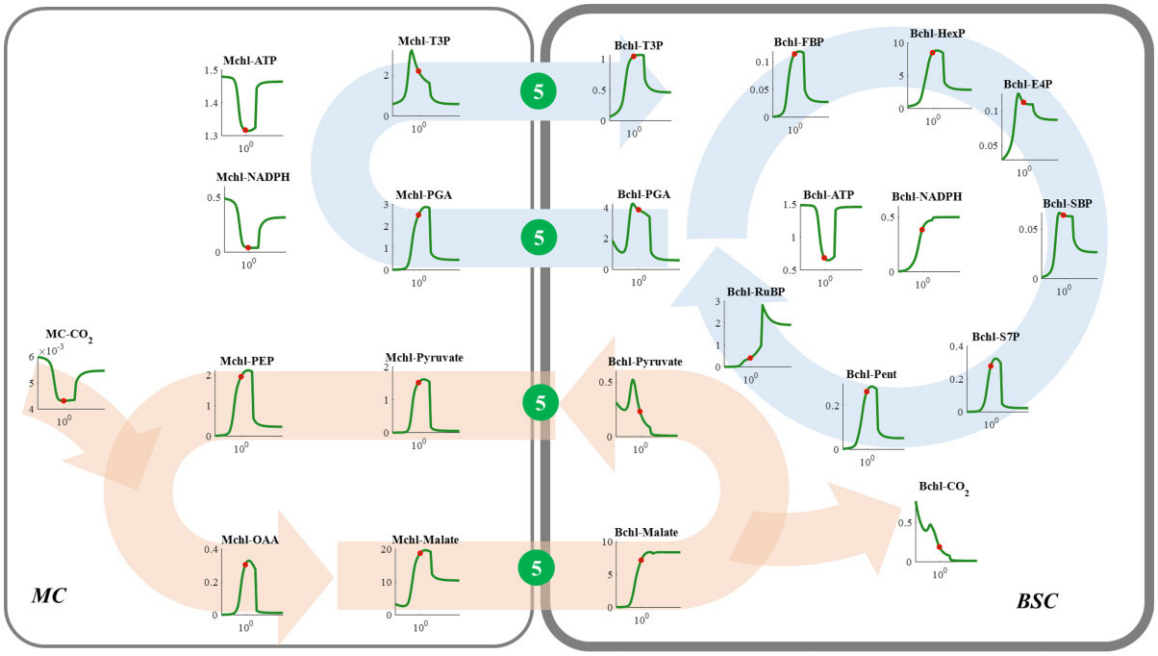

Figure 8 Responses of metabolite levels in NADP-ME type C_4 photosynthetic metabolism to the Plasmodesmata (the dark green circle numbered ⑤) proportion. See figure legend for Figure 4 for more details.

inhibited photosynthesis at a high plasmodesmata area proportion was not caused by the changed level of RuBP in BSC (Figures 3, I and 8), but rather the changed CO_2 levels (Figures 3, J and 8); this is because RuBP levels at high plasmodesmata area proportion conditions were always larger than those under the optimum condition (Figure 8). The excessive plasmodesmata area proportion, however, resulted in a decreased CO_2 concentration and low concentrations of other intermediates in the CBC, except ATP and NADPH (Figure 8). Concurrently, levels of all the metabolites in the C_4 cycle were also decreased when the plasmodesmata area proportion was higher than the optimum, except for malate levels in BSC (Figure 8).

Changes in metabolite levels in the C_3 metabolism affect CCM metabolism through influencing PGA concentration and redox levels

When we perturbed the enzyme activities in the C_3 metabolism, PGA concentrations in the Mchl were affected by PGAK in the Mchl (Figure 4) and enzymes of the CBC in the Bchl (Figures 5–7). When the PGA concentration was perturbed, we found that the PEP concentrations have the same pattern of changes as that of Mchl PGA (Figures 4–8) in all simulations.

In some perturbations (Figures 5–8), both PGA and PEP concentrations decreased. However, malate accumulated to a high level and the CO_2 concentration around Rubisco is low (Figures 5–8), which indicates the CCM is mainly limited by a low decarboxylation of NADP-ME. Since the enzyme activity and kinetic properties of NADP-ME were not changed in our perturbations (Figures 4–8), the decreased NADP-ME flux could only be caused by decreased substrate concentrations. Considering that the malate level was high, the limitation is caused by a low $NADP^+$ (Hatch and Kagawa, 1976). In our model, the total content of NADPH and $NADP^+$ is assumed as a constant in the Bchl ($[NADP^+]$ + [NADPH] = 0.5 mM; Wang et al., 2014a, 2014b). In our simulation, the high malate concentration and low CO_2 concentration in the Bchl were accompanied by a high NADPH concentration (near to 0.5 mM; Figures 5–8) and low $NADP^+$ level. Therefore, a suitable redox potential in the Bchl is required for malate decarboxylation in the Bchl.

Discussion

Many features and required elements for an efficient NADP-ME type C_4 photosynthesis (Wang et al., 2014a, 2014b; von Caemmerer and Furbank, 2016) have been discovered previously, which include sufficient capacities for enzymes and transporters involved in the C_4 shuttle, sufficient capacity for RuBP regeneration, sufficient Rubisco capacity in the BSC, and sufficient electron transfer capacity in the MC and BSC for ATP and NADPH generation. These features are basic elements required for an efficient operation of C_4 photosynthesis. This study quantitatively demonstrates that two additional mechanisms are required to effectively coordinate the C_3 metabolism and C_4 shuttle for a higher C_4 photosynthetic efficiency (Figure 9). These two routes include (1) building up the PEP concentration through maintaining the PGA content in the MC to ensure substrate supply for the PEPC catalyzed reaction and (2) maintaining a suitable oxidation state in the BSC to enable an efficient malate decarboxylation via NADP-ME.

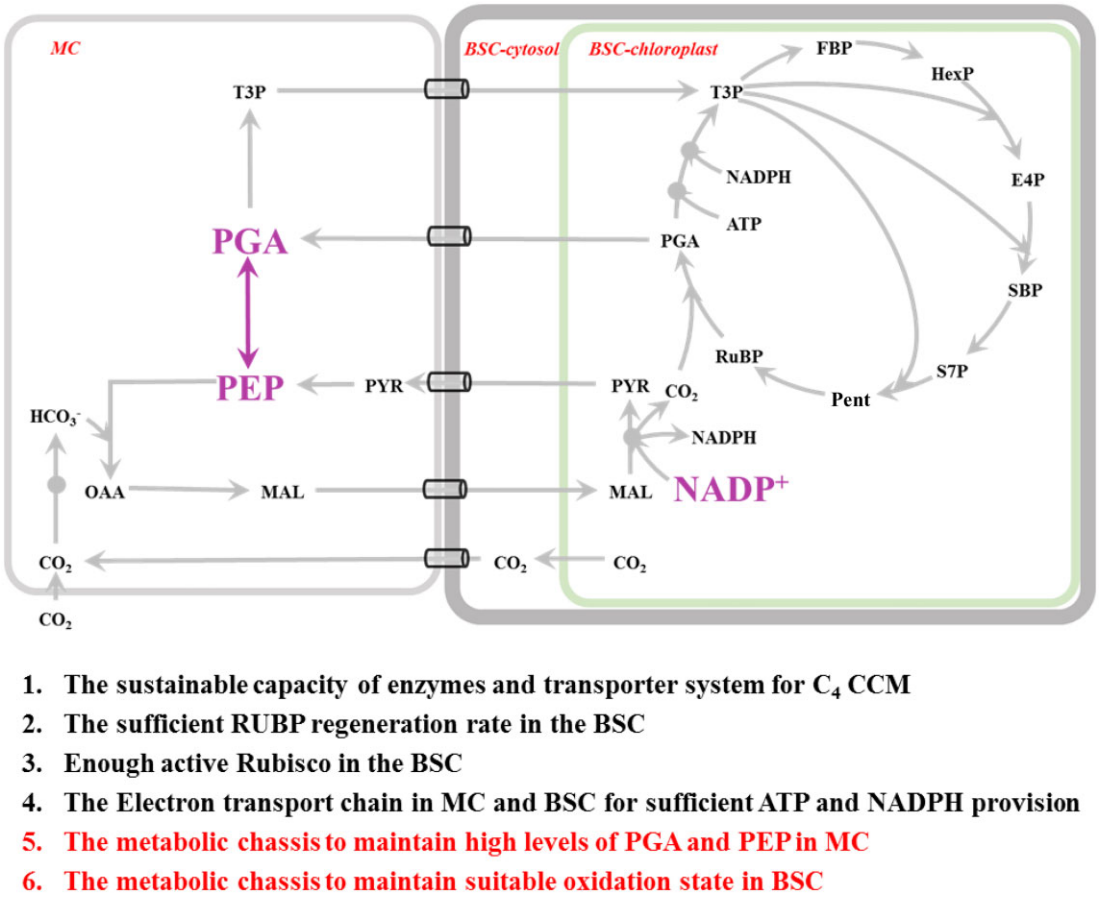

Figure 9 The requirements for an efficient NADP-ME type C_4 photosynthesis. In addition to the known elements for an efficient NADP-ME type C_4 photosynthesis (1–4 in black; Wang et al., 2014a, 2014b; von Caemmerer and Furbank, 2016), maintaining high concentrations of PGA and PEP in mesophyll chloroplasts and a high concentration of $NADP^+$ in Bchl are also required to gain high C_4 flux (5 and 6 in red). These two additional biochemical requirements are present in purple and with the larger font size in the graph.

Building up the PEP concentration by maintaining the PGA concentration in the Mchl is required for an efficient PEPC catalyzed carboxylation

The reactions catalyzed by FBPA, FBPase, and PGAK-GAPDH in the Bchl can influence RuBP regeneration in C_4 photosynthesis (Figure 2), which is similar to their effects on C_3 photosynthesis (Zhao et al., 2020). In C_4 photosynthesis, not only the RuBP regeneration but also the CCM efficiency is affected by PGAK-GAPDH, FBPA, and FBPase (Figures 5–7). These results demonstrate the C_4 cycle interacts closely with C_3 metabolism and the coordination between them is critical for an efficient NADP-ME type C_4 photosynthesis.

For the NADP-ME type of C_4 CCM, the C_4 cycle functions as a pump to concentrate CO_2 around Rubisco in the BSC. Meanwhile, the reducing power is released during malate decarboxylation as NADPH which is stoichiometrically equal to the CO_2 release rate. Two NADPH molecules are needed to fix one molecule of CO_2 through the CBC in the BSC. The NADPH needed for CO_2 assimilation in the BSC can be replenished from the BSC chloroplastic electron transport chain and the PGA/T3P shuttled from the MC (Hatch, 1987). The replenishment of BSC NADPH shuttled from MC rather than the direct generation within BSC is a strategy due to the decreased level of photosystem II (PSII) in Bchls (Hatch, 1987) and the limited capacity of electron transfer from water to $NADP^+$ as observed in maize (Hatch and Kagawa, 1976). In a typical NADP-ME type C_4 photosynthesis, during the processes of shuttling NADPH from MC, a portion of PGA produced by RuBP carboxylation is transported from BSC to MC, where it is reduced to T3P in the Mchl; thereafter, the T3P is transported back from MC to BSC and further as the intermediates of the CBC in the BSC (Huber and Edwards, 1975). Consistent with this, low concentration of PGA in the MC is unfavorable for ATP and NADPH replenishment from MC to BSC in the NADP-ME type of C_4 photosynthesis (Hatch and Kagawa, 1976; Leegood and von Caemmerer, 1988; Wang et al., 2014a, 2014b).

Furthermore, PGA in the Mchl can not only function as the substrate of PGAK, but can also be reversibly converted to produce PEP by two reversible enzymes (Huber and Edwards, 1975). In our simulations, PEP and PGA contents always change synchronously under different perturbations (Figures 4–8). These results are consistent with those reported in previous studies in which PEP and PGA contents change synchronously under different environmental

conditions in various C_4 plants (Leegood and von Caemmerer, 1988, 1989). It indicates that the C_4 cycle and C_3 metabolism are closely linked due to the reversible conversions between PGA and PEP (von Caemmerer and Furbank, 2016). As a result, the disruption of coordination in CBC which leads to either a decrease in PGA production or the over-consumption of PGA can decrease PGA and PEP concentrations simultaneously, and ultimately suppressed CO_2 fixation by PEPC and correspondingly decreased the downstream metabolites in the C_4 cycle (Figures 2–8). With the interconversions between PEP and PGA, it seems difficult to build up the PEP content completely dependent on PEP regeneration through the C_4 cycle. In other words, to support enough substrate PEP as the donor of CO_2 fixation via PEPC, it is required to build up the high level of PEP in the MC through maintaining a high PGA concentration.

In the C_4 rice engineering, the flux of CO_2 fixation by PEPC was increased within C_4 transgenic rice (Lin et al., 2020; Ermakova et al., 2021), but the flux of PEPC in transgenic rice was only 2% of that in maize (Ermakova et al., 2021). This might be the result of the low activity of PEPC (Lin et al., 2020; Ermakova et al., 2021) and the low PEP concentration in the transgenic rice plants (Fukayama et al., 2003; Ermakova et al., 2021). Both the content of PEP and PGA in rice are much lower than that in maize (Fukayama et al., 2003; Arrivault et al., 2019). Considering that the affinity of leaf PEPC for PEP in maize (K_m = 1.48 mM) is much lower than that in rice (K_m = 0.1–0.12 mM; Masumoto et al., 2010, 2015), besides the PEPC activity, gaining a high PEP concentration is also required for an efficient operation of C_4 type PEPC. Therefore, it is needed to maintain a high PGA concentration in MC to support an efficient NADP-ME type C_4 photosynthesis.

In a typical C_3 MC, five-sixths of PGA is metabolized for RuBP regeneration and near a half of net produced PGA is used for starch synthesis (Szecowka et al., 2013). Different from that, in NADP-ME type C_4 plants, except the PGAK, GAPDH, and TPI, the other CBC enzymes are mainly located in the Bchl (Schlüter and Weber, 2020), and starch synthesis is usually located in Bchl where the CBC is located (Lunn and Furbank, 1997). This localization of starch synthesis and most of the CBC cycle in the BSC may help maintain a high concentration of PGA in the MC, in addition to the recognized role of transferring reducing equivalent and ATP from MC to BSC (Wang et al., 2014a, 2014b). Consistently, our predictions show that further increasing activities of Aldolase and FBPase in MC cytosol to consume more T3P and PGA for sucrose synthesis can also decrease C_4 photosynthesis (Supplemental Figure S1), as a result of their impacts on PGA, T3P, and PEP levels (Supplemental Figure S2) in the MC. In C_4 rice engineering, to build up the PEP concentration through maintaining PGA concentration, downregulation of the whole fluxes of CBC and starch synthesis in the MC to reduce the consumption of PGA in MC might be important strategies.

Maintaining a suitable redox status in Bchls is required for efficient NADP-ME photosynthesis

Another observation from this study is that CO_2 may still become a limiting factor for photosynthesis even when the malate concentration is high (Figures 5 and 8), which reflects a limitation of malate decarboxylation by the availability of $NADP^+$. In our simulations, a high level of malate is accompanied with an accumulation of NADPH in the Bchl (Figures 5 and 8), which is consistent with the previous study which proposed that the oxidation state of the chloroplast is the driver of NADP-ME catalyzed malate decarboxylation (Bräutigam et al., 2018).

The lack of $NADP^+$ can lead to a low efficiency of malate decarboxylation and correspondingly a low efficiency of photosynthesis itself. To date, in the C_4 rice engineering project, levels of all enzymes belonging to the NADP-ME CCM pathway have been successfully increased in transgenic rice, and this increases the fluxes of CO_2 fixation by PEPC to produce aspartate and malate (Lin et al., 2020; Ermakova et al., 2021). However, the malate decarboxylation flux through NADP-ME is undetectable (Lin et al., 2020; Ermakova et al., 2021). A number of factors have been proposed to contribute to this lack of decarboxylation fluxes. First, this might be due to a low level of NADP-ME expression in transgenic plants (Lin et al., 2020; Ermakova et al., 2021). Second, lack of transporters required for the NADP-ME CCM and the incorrect location of enzymes might contribute to the lack of fluxes (Lin et al., 2020). Third, results from this study suggest that the lack of sufficient flux might also be due to a shortage of $NADP^+$ for malate decarboxylation (Figures 5 and 8). This might be the case in the study of Tsuchida et al. (2001), who constructed transgenic rice plants with increased NADP-ME activity up to 30-fold of that in WT plants; however, the enhanced NADP-ME activity in rice resulted in photoinhibition and retarded plant growth (Tsuchida et al., 2001).

What might be the strategies to maintain a more oxidized redox status in BSC? First, mixed decarboxylation types exist in almost all the natural C_4 plants (Furbank, 2011), which might contribute to establishment of an appropriate redox status (Stitt and Zhu, 2014; Wang et al.,2014a, 2014b). This agrees with the observation that, feeding exogenous aspartate increases the rate of light-dependent malate decarboxylation in the BSC of maize leaf without increasing NADP-ME activity (Chapman and Hatch, 1979). In addition to maintaining the suitable redox status, the mixed strategy can also decrease the demand for maintaining high concentrations of a particular C_4 acid for an efficient C_4 photosynthesis (Pick et al., 2011; Wang et al., 2014a, 2014b). Besides using a mixed pathway, in NADP-ME type C_4 plants, the reduced PSII content in the BSC might be another strategy to generate a more oxidized status (Leegood et al., 1981; Nakamura et al., 2013; von Caemmerer and Furbank, 2016; Ermakova et al., 2020).

Summary

In the current effort of either improving C_4 photosynthesis or engineering C_3 plants to perform C_4 photosynthesis, the

Kranz anatomy, the capacities of enzymes, transporters, diffusion across plasmodesmata, and electron transport chain are considered as the major elements for an efficient C_4 CCM (von Caemmerer and Furbank, 2016; Ermakova et al., 2020). Evidence from this quantitative simulation study shows that, besides these known requirements, maintaining high levels of PGA in MC and a suitable oxidized status in the Bchl are also required features for an efficient NADP-ME type C_4 CCM. Potential strategies in C_4 leaves to maintain a high PGA level in the MC include (1) constraining the starch synthesis pathway into the BSC and (2) decreasing the fluxes of the whole CBC in MC. The potential strategies to maintain a suitable oxidized status in the BSC include the mixed decarboxylases, maintaining minimal or no PSII activity in the BSC, and other factors discussed previously (Stitt and Zhu, 2014). More experimental studies are still needed to test these predicted features on improving C_4 photosynthetic efficiency and engineering C_4 rice.

Materials and methods

Parameter perturbations

The dynamic model of NADP-ME type C_4 photosynthesis based on the Michaelis–Menten equation constructed previously (Wang et al., 2014a, 2014b) was used as a basis for our analysis. The model includes the metabolic pathways related to the NADP-ME type CCM which includes the CBC in the BSC, sucrose synthesis in the MC and starch synthesis in the BSC, photorespiration and the NADP-ME type C_4 shuttle process. The transporters located on the chloroplast membrane mediating metabolite translocation between chloroplast and cytosol, and transporters located on the plasmodesmata linking BSC and MC for metabolites diffusion are also included (Wang et al., 2014a, 2014b). In this study, all the initial maximum velocities of the enzymes were the default values assigned in the previous model (Wang et al., 2014a, 2014b), in which the values of parameters were collected mostly for maize (*Z. mays*). The main structure has been simplified and redrawn in this study (Figures 1 and 2, A). The default maximal velocities of all enzymes (V_{max}(s) of 36 enzymes) and parameters of plasmodesmata, that is, the area proportion and length, were perturbated with a range of fold change between 0.01 and 1,000. In each simulation, we only perturbed one parameter with all other parameters maintaining their default values. All the simulations were performed using MATLAB (2012). The method of perturbations is the same as (Zhao et al., 2020).

Supplemental data

The following materials are available in the online version of this article.

Supplemental Figure S1. The response curves of photosynthesis to the fold changes of enzymatic capacity.

Supplemental Figure S2. The response curves of PGA, T3P, and PEP to the fold changes of enzymatic capacity.

Acknowledgments

We thank Prof. Genyun Chen, Ms. Fenfen Miao, and Xinyu Liu for editing the manuscript and for the project discussion. We acknowledge Prof. Steve Long, Dr. Yi Xiao, Mark Stitt, Rowan Sage, John Lunn, and all members of plant systems biology group in CEMPS, of C_4 rice consortium and of RIPE team for the valuable suggestions.

Funding

This work was supported by grants from the Ministry of Science and Technology of China (2019YFA09004600 and 2020YFA0907604), from the Chinese Academy of Sciences strategic leading project (XDB27020105), from the general program of the National Natural Sciences Foundation of China (31870214 and 31701139), from the Bill & Melinda Gates Foundation to the University of Oxford (OPP1129902), and from the Bill & Melinda Gates Foundation (OPP1172157).

Conflict of interest statement. The authors have no conflicts of interest to report.

References

Antonovsky N, Gleizer S, Noor E, Zohar Y, Herz E, Barenholz U, Zelcbuch L, Amram S, Wides A, Tepper N, et al. (2016) Sugar synthesis from CO2 in Escherichia coli. Cell **166:** 115–125

Arrivault S, Alexandre Moraes T, Obata T, Medeiros DB, Fernie AR, Boulouis A, Ludwig M, Lunn JE, Borghi GL, Schlereth A, et al. (2019) Metabolite profiles reveal interspecific variation in operation of the Calvin-Benson cycle in both C-4 and C-3 plants. J Exp Bot **70:** 1843–1858

Barenholz U, Davidi D, Reznik E, Bar-On Y, Antonovsky N, Noor E, Milo R (2017) Design principles of autocatalytic cycles constrain enzyme kinetics and force low substrate saturation at flux branch points. eLife **6**: e20667

Boyd RA, Gandin A, Cousins AB (2015) Temperature responses of C_4 photosynthesis: biochemical analysis of rubisco, phospho*enol*-pyruvate carboxylase, and carbonic anhydrase in *Setaria viridis*. Plant Physiol **169:** 1850–1861

Bräutigam A, Schlüter U, Lundgren M, Flachbart S, Ebenhöh O, Schönknecht G, Christin P, Bleuler S, Droz J, Osborne C, et al. (2018) Biochemical mechanisms driving rapid fluxes in C_4 photosynthesis. bioRxiv. 387431, https://doi.org/10.1101/387431

Brown RH, Bouton JH (1993) Physiology and genetics of interspecific hybrids between photosynthetic types. Ann Rev Plant Physiol Plant Mol Biol **44:** 435–456

Chapman KSR, Hatch MD (1979) Aspartate stimulation of malate decarboxylation in *Zea mays* bundle sheath cells: possible role in regulation of C4 photosynthesis. Biochem Biophys Res Commun **86:** 1274–1280

Covshoff S, Hibberd JM (2012) Integrating C_4 photosynthesis into C_3 crops to increase yield potential. Curr Opin Biotechnol **23:** 209–214

Ermakova M, Arrivault S, Giuliani R, Danila F, Alonso-Cantabrana H, Vlad D, Ishihara H, Feil R, Guenther M, Borghi GL, et al. (2021) Installation of C_4 photosynthetic pathway enzymes in rice using a single construct. Plant Biotechnol J **19:** 575–588

Ermakova M, Danila FR, Furbank RT, Von Caemmerer S (2020) On the road to C_4 rice: advances and perspectives. Plant J **101:** 940–950

Farquhar GD, von Caemmerer S, Berry JA (1980) A biochemical model of photosynthetic CO2 assimilation in leaves of C 3 species. Planta **149** 78–90

Fendt SM, Buescher JM, Rudroff F, Picotti P, Zamboni N, Sauer U (2010) Tradeoff between enzyme and metabolite efficiency maintains metabolic homeostasis upon perturbations in enzyme capacity. Mol Syst Biol **6:** 356

Fukayama H, Hatch MD, Tamai T, Tsuchida H, Sudoh S, Furbank RT, Miyao M (2003) Activity regulation and physiological impacts of maize C_4 -specific phosphoenolpyruvate carboxylase overproduced in transgenic rice plants. Photosynth Res **77:** 227–239

Fukayama H, Tamai T, Taniguchi Y, Sullivan S, Miyao M, Nimmo HG (2006) Characterization and functional analysis of phosphoenolpyruvate carboxylase kinase genes in rice. Plant J **47:** 258–268

Fukayama H, Tsuchida H, Agarie S, Nomura M, Onodera H, Ono K, Lee BH, Hirose S, Toki S, Ku MS, et al. (2001) Significant accumulation of C_4 -specific pyruvate, orthophosphate dikinase in a C_3 plant, rice. Plant Physiol **127:** 1136–1146

Furbank RT (2011) Evolution of the C_4 photosynthetic mechanism: are there really three C_4 acid decarboxylation types? J Exp Bot **62:** 3103–3108

Furbank RT, Quick WP, Sirault XRR (2015) Improving photosynthesis and yield potential in cereal crops by targeted genetic manipulation: Prospects, progress and challenges. Field Crop Res **182:** 19–29

Hatch MD (1987) C_4 photosynthesis: a unique elend of modified biochemistry, anatomy and ultrastructure. Biochim Biophys (BBA)-Rev Bioenerget **895:** 81–106

Hatch MD, Kagawa T (1976) Photosynthetic activities of isolated bundle sheath cells in relation to differing mechanisms of C_4 pathway photosynthesis. Arch Biochem Biophys **175:** 39–53

Hibberd JM, Sheehy JE, Langdale JA (2008) Using C_4 photosynthesis to increase the yield of rice - rationale and feasibility. Curr Opin Plant Biol **11:** 228–231

Huber SC, Edwards GE (1975) Regulation of oxaloacetate, aspartate, and malate formation in mesophyll protoplast extracts of three types of C_4 plants. Plant Physiol **56:** 324–331

Hunter MC, Smith RG, Schipanski ME, Atwood LW, Mortensen DA (2017) Agriculture in 2050: recalibrating targets for sustainable intensification. BioScience **67:** 386–391

Khozaei M, Fisk S, Lawson T, Gibon Y, Sulpice R, Stitt M, Lefebvre SC, Raines CA (2015) Overexpression of plastid transketolase in tobacco results in a thiamine auxotrophic phenotype. Plant Cell **27:** 432–447

Ku MS, Cho D, Li X, Jiao DM, Pinto M, Miyao M, Matsuoka M (2001) Introduction of genes encoding C_4 photosynthesis enzymes into rice plants: physiological consequences. Novartis Found Symp **236:** 100–111; discussion 111–106

Leegood RC, Crowther D, Walker DA, Hind G (1981) Photosynthetic electron-transport in the bundle sheath of maize. FEBS Lett **126:** 89–92

Leegood RC, von Caemmerer S (1988) The relationship between contents of photosynthetic metabolites and the rate of photosynthetic carbon assimilation in leaves of amaranthus-edulis L. Planta **174:** 253–262

Leegood RC, von Caemmerer S (1989) Some relationships between contents of photosynthetic intermediates and the rate of photosynthetic carbon assimilation in leaves of zea-mays-L. Planta **178:** 258–266

Lin HC, Arrivault S, Coe RA, Karki S, Covshoff S, Bagunu E, Lunn JE, Stitt M, Furbank RT, Hibberd JM, et al. (2020) A partial C4 photosynthetic biochemical pathway in rice. Front Plant Sci **11**: 564463

Long SP, Marshall-Colon A, Zhu XG (2015) Meeting the global food demand of the future by engineering crop photosynthesis and yield potential. Cell **161:** 56–66

López-Calcagno PE, Brown KL, Simkin AJ, Fisk SJ, Vialet-Chabrand S, Lawson T, Raines CA (2020) Stimulating photosynthetic processes increases productivity and water-use efficiency in the field. Nat Plants **6:** 1054–1063

Lunn JE, Furbank RT (1997) Localisation of sucrose-phosphate synthase and starch in leaves of C4 plants. Planta **202:** 106–111

Masumoto C, Miyazawa S, Ohkawa H, Fukuda T, Taniguchi Y, Murayama S, Kusano M, Saito K, Fukayama H, Miyao M (2010) Phosphoenolpyruvate carboxylase intrinsically located in the chloroplast of rice plays a crucial role in ammonium assimilation. Proc Natl Acad Sci USA **107:** 5226–5231

Matsuoka M, Furbank RT, Fukayama H, Miyao M (2001) Molecular engineering of C_4 photosynthesis. Ann Rev Plant Physiol Plant Mol Biol **52:** 297–314

Miyao M, Masumoto C, Miyazawa SI, Fukayama H (2011) Lessons from engineering a single-cell C_4 photosynthetic pathway into rice. J Exp Bot **62:** 3021–3029

Muramatsu M, Suzuki R, Yamazaki T, Miyao M (2015) Comparison of plant-type phosphoenolpyruvate carboxylases from rice: identification of two plant-specific regulatory regions of the allosteric enzyme. Plant Cell Physiol **56:** 468–480

Nakamura N, Iwano M, Havaux M, Yokota A, Munekage YN (2013) Promotion of cyclic electron transport around photosystem I during the evolution of NADP-malic enzyme-type C_4 photosynthesis in the genus Flaveria. New Phytol **199:** 832–842

Pick TR, Bräutigam A, Schlüter U, Denton AK, Colmsee C, Scholz U, Fahnenstich H, Pieruschka R, Rascher U, Sonnewald U, et al. (2011) Systems analysis of a maize leaf developmental gradient redefines the current C4 model and provides candidates for regulation. Plant cell **23:** 4208–4220

Ray DK, Mueller ND, West PC, Foley JA (2013) Yield Trends Are Insufficient to Double Global Crop Production by 2050. PLoS One **8:** e66428

Sage RF (2004) The evolution of C_4 photosynthesis. New Phytologist **161:** 341–370

Salesse-Smith CE, Sharwood RE, Busch FA, Kromdijk J, Bardal V, Stern DB (2018) Overexpression of Rubisco subunits with RAF1 increases Rubisco content in maize. Nat Plants **4:** 802–810

Schlüter U, Weber APM (2020) Regulation and evolution of C_4 photosynthesis. Ann Rev Plant Biol **71**: 183–215

Shen BR, LM, Lin XL, Yao Z, Xu HW, Zhu CH, Teng HY, Cui LL, Liu EE, Zhang JJ, et al. (2019) Engineering a new chloroplastic photorespiratory bypass to increase photosynthetic efficiency and productivity in rice. Mol Plant **12:** 199–214

South PF, Cavanagh AP, Liu HW, Ort DR (2019) Synthetic glycolate metabolism pathways stimulate crop growth and productivity in the field. Science **363:** eaat9077

Stitt M, Zhu XG (2014) The large pools of metabolites involved in intercellular metabolite shuttles in C_4 photosynthesis provide enormous flexibility and robustness in a fluctuating light environment. Plant Cell Environ **37:** 1985–1988

Studer AJ, Gandin A, Kolbe AR, Wang L, Cousins AB, Brutnell TP (2014) A limited role for carbonic anhydrase in C_4 photosynthesis as revealed by a *ca1ca2* double mutant in maize. Plant Physiol **165:** 608–617

Szecowka M, Heise R, Tohge T, Nunes-Nesi A, Vosloh D, Huege J, Feil R, Lunn J, Nikoloski Z, Stitt M, et al. (2013) Metabolic Fluxes in an Illuminated Arabidopsis Rosette. Plant Cell **25:** 694–714

Taniguchi Y, Ohkawa H, Masumoto C, Fukuda T, Tamai T, Lee K, Sudoh S, Tsuchida H, Sasaki H, Fukayama H, et al. (2008) Overproduction of C_4 photosynthetic enzymes in transgenic rice plants: an approach to introduce the C4-like photosynthetic pathway into rice. J Exp Bot **59:** 1799–1809

Tsuchida H, Tamai T, Fukayama H, Agarie S, Nomura M, Onodera H, Ono K, Nishizawa Y, Lee BH, Hirose S, et al. (2001) High level expression of C_4-specific NADP-malic enzyme in leaves and impairment of photoautotrophic growth in a C_3 plant, rice. Plant Cell Physiol **42:** 138–145

von Caemmerer S, Furbank RT (2016) Strategies for improving C_4 photosynthesis. Curr Opin Plant Biol **31:** 125–134

von Caemmerer S, Millgate A, Farquhar GD, Furbank RT (1997) Reduction of ribulose-1,5-bisphosphate carboxylase/oxygenase by antisense RNA in the C_4 plant flaveria bidentis leads to reduced assimilation rates and increased carbon isotope discrimination. Plant Physiol **113:** 469–477

von Caemmerer S, Quinn V, Hancock NC, Price GD, Furbank RT, Ludwig M (2004) Carbonic anhydrase and C_4 photosynthesis: a transgenic analysis. Plant Cell Environ **27:** 697–703

Wang DF, Portis AR, Moose SP, Long SP (2008) Cool C_4 photosynthesis: Pyruvate P_i dikinase expression and activity corresponds to the exceptional cold tolerance of carbon assimilation in *Miscanthus x giganteus*. Plant Physiol **148:** 557–567

Wang Y, Brautigam A, Weber AP, Zhu XG (2014a) Three distinct biochemical subtypes of C_4 photosynthesis? A modelling analysis. J Exp Bot **65:** 3567–3578

Wang Y, Long SP, Zhu XG (2014b) Elements required for an efficient NADP-malic enzyme type C_4 photosynthesis. Plant Physiol **164:** 2231–2246

Zhao H, Tang Q, Chang T, Xiao Y, Zhu XG (2020) Why an increase in activity of an enzyme in the Calvin Benson Cycle does not always lead to an increased photosynthetic CO2 uptake rate? – A theoretical analysis. In silico Plants

Zhu XG, Long SP, Ort DR (2008) What is the maximum efficiency with which photosynthesis can convert solar energy into biomass? Curr Opin Biotechnol **19:** 153–159